Crystal structure of an Aurora-A mutant that mimics Aurora-B bound to MLN8054: insights into selectivity and drug design

Charlotte A Dodson, Magda Kosmopoulou, Mark W Richards, Butrus Atrash, Vassilios Bavetsias, Julian Blagg, Richard Bayliss

Crystal structure of an Aurora-A mutant that mimics Aurora-B bound to MLN8054: insights into selectivity and drug design

Charlotte A Dodson[1,†], Magda Kosmopoulou[1,†], Mark W Richards[1], Butrus Atrash[2], Vassilios Bavetsias[2], Julian Blagg[2], Richard Bayliss[1]*

1. Section of Structural Biology, The Institute of Cancer Research, Chester Beatty Laboratories, 237 Fulham Road, London, SW3 6JB, United Kingdom.
2. Cancer Research UK Centre for Cancer Therapeutics, The Institute of Cancer Research, Haddow Laboratories, 15 Cotswold Road, Sutton, Surrey SM2 5NG, United Kingdom.
† Contributed equally to this work.
*** Corresponding Author**
Contact details of the corresponding author:
Phone: +44 (0)207 1535557
Fax: +44 (0)207 1535457
Email richard.bayliss@icr.ac.uk

Running Title
Aurora-A/MLN8054 crystal structure

Keywords
Aurora-A kinase, MLN8054, DFG-in, DFG-up, DFG-out, drug design, inhibitor selectivity

Abbreviations used: ePK, eukaryotic protein kinase; ESRF, European Synchrotron Radiation Facility; FAM, carboxyfluorescein; K_i, dissociation constant for inhibitor; PDB, Protein Data Bank; PEG, polyethylene glycol; TPX2, targeting protein for Xenopus Xklp2.

ABSTRACT

The production of selective protein kinase inhibitors is often frustrated by the similarity of the enzyme active sites. For this reason, it is challenging to design inhibitors that discriminate between the three Aurora kinases, which are important targets in cancer drug discovery. We have used a triple point mutant of Aurora-A ($AurA^{x3}$) that mimics the active site of Aurora-B to investigate the structural basis of MLN8054 selectivity. The bias toward Aurora-A inhibition by MLN8054 is fully recapitulated by $AurA^{x3}$ *in vitro*. X-ray crystal structures of the complex suggest that the basis for the discrimination is electrostatic repulsion due to the Thr217Glu substitution, which we have confirmed using a single point mutant. The activation loop of Aurora-A in the $AurA^{x3}$/MLN8054 complex exhibits an unusual conformation in which Asp274 and Phe275 sidechains point into the interior of the protein. There is to our knowledge no documented precedent for this conformation, which have termed DFG-up. The sequence requirements of the DFG-up conformation suggest that it might be accessible to only a fraction of kinases. MLN8054 thus circumvents the problem of highly homologous active sites. Binding of MLN8054 to Aurora-A switches the character of a pocket within the active site from polar to hydrophobic pocket, similar to what is observed in the structure of Aurora-A bound to a compound that induces DFG-out. We propose that targeting this pocket may be a productive route in the design of selective kinase inhibitors and describe the structural basis for the rational design of these compounds.

INTRODUCTION

Following the success of Glivec in the treatment of chronic myelogenous leukaemia, the development of small molecule kinase inhibitors has become an established goal in drug discovery [1]. A major obstacle is that the ATP binding pocket, the ubiquitous druggable binding site for inhibitors, is highly conserved across more than 500 human kinases. The rapid growth in the number and chemical variety of kinase inhibitors has been aided by the contribution of structural biology especially the high resolution snapshots of kinase/inhibitor complexes captured by X-ray crystallography [1, 2]. These studies revealed the specific conformations recognized by the two main classes of kinase inhibitor. Type I inhibitors recognize the active, typically phosphorylated, form of the kinase, and Type II inhibitors recognize an inactive, typically dephosphorylated form of the enzyme. In Type I inhibitor co-crystal structures, the conformation of the activation loop, a motif containing the regulatory phosphorylation sites of kinases, adopts the same conformation as that observed in ADP/ATP-bound structures. This conformation is termed DFG-in after the highly conserved aspartic acid, phenylalanine, glycine motif at the N-terminus of the activation loop. In the DFG-in conformation, the aspartic acid sidechain points into the active site where it coordinates divalent cations and the phenylalanine sidechain points into the interior of the protein. By contrast, Type II compounds stabilize a DFG-out conformation of the activation loop, in which the phenylalanine sidechain points outwards and interacts with the compound and the aspartic acid sidechain is displaced away from the active site [3-5]. Structure-based drug design can be used to develop Type II, DFG-out binding compounds based on Type I, DFG-in binding precursors [6]. The field is still a long way from the direct rational design of selective and potent kinase inhibitors with a controlled selectivity profile. Currently, multiple iterative design cycles are

required to optimise compounds towards the desired biological profile. However, structural biology has provided insight and direction to the design of selective inhibitors that avoid off-target kinases. The selectivity profile of kinase inhibitors is very difficult to explain, even with the help of a high-resolution crystal structure. For example, nine years after the crystal structure of cAbl bound to a Glivec variant showed that this inhibitor recognizes the DFG-out conformation, there is still debate about the structural and thermodynamic basis for its selectivity [3, 7, 8]. It is clear, however, that the cAbl/Glivec variant structure was the inspiration for a new approach to kinase inhibitor design that has yielded many valuable compounds [6].

Many mitotic kinases are promising cancer drug targets because they are overexpressed in tumours, and their inhibition generates an aberrant cell division that can selectively kill tumour cells [9]. A great deal of attention has been focused on the three Aurora kinases (A, B and C), and a number of structurally diverse inhibitors have been developed that target this family [10-12]. The Millennium Pharmaceuticals compound MLN8054 is an Aurora-family specific inhibitor that inhibits 7 out of 226 kinases more than 50% at a concentration of 1 μM [13] or has a K_d < 100 nM for 6 out of 317 kinases [14]. Unlike any of the other Aurora inhibitors, MLN8054 is based on a benzazepine scaffold and it has been of considerable interest to determine the binding mode of this compound and shed light on its specificity. MLN8054 is also the first inhibitor discovered to show increased selectivity towards Aurora-A both in a human colorectal tumour cell-line and *in vitro* [13, 14]. Aurora-A is amplified and/or overexpressed in many cancers and cancer cell lines including hepatocellular carcinoma [15], breast cancers [16] and neuroblastoma cell lines [16]. Polymorphisms in the Aurora-A gene confer increased breast and colon tumour susceptibility and somatic mutations in Aurora-A have been identified in colorectal adenocarcinoma, lung carcinoma and melanoma [17, 18]. Inhibition of Aurora-A may be a useful therapeutic strategy in these cancers, and clinical trials of several Aurora inhibitors, including a modified version of MLN8054 (MLN8237) are ongoing.

The selectivity of MLN8054 can be considered as a function of two individual factors: bias towards Aurora-A, and selectivity towards the Aurora family. To investigate the first factor, we have studied the effects of MLN8054 on both Aurora-A and an Aurora-B active-site mimic ($AurA^{x3}$). We find that MLN8054 exhibits a 6-fold stronger inhibition of Aurora-A than $AurA^{x3}$ *in vitro*. The crystal structure of $AurA^{x3}$ bound to MLN8054 exhibits a highly unusual conformation of the activation loop. The characteristic features of the conformation are that both the aspartic acid and phenylalanine residues of the DFG motif point into the interior of the protein structure, and the activation loop wraps around the inhibitor and makes contact using a valine sidechain five residues after the start of the DFG motif. The structural details of this conformation, and a comparison of the key residues involved with those found in other human kinases show that it provides a rationale for understanding the selectivity of MLN8054 towards Aurora kinases. The binding of MLN8054 is accompanied by the creation of a hydrophobic pocket equivalent to that filled by the DFG Phe sidechain in a DFG-out structure. Our analysis suggests that a subset of kinases could be targeted through the design of inhibitors to fill this pocket, and that this would be an alterative route to producing highly specific compounds.

MATERIALS AND METHODS

Chemical synthesis
MLN8054 was synthesized as previously described [19].

Protein production and crystallization
The Quikchange (Stratagene) method of site-specific mutagenesis was used to produce AurA^{x3} (Leu215Arg, Thr217Glu and Arg220Lys), AurA^{TE} (Thr217Glu) and AurA^{WL} (Trp277Leu). AurA, AurA^{x3}, AurA^{TE} and AurA^{WL} proteins were expressed and purified as previously [20]. Crystals of AurA^{x3}/MLN8054 were obtained using the hanging drop method of vapour diffusion. For the $P3_1$ form, the well buffer was 0.8 M NaH_2PO_4/1.2 M K_2HPO_4 and 0.1 M acetate, pH 4.5. For the $P6_122$ form, the well buffer was 0.1 M Mes sodium salt pH 6.5, 2.0 M ammonium sulfate, 5% (w/v) PEG400. Drops comprised a 1:1 ratio of AurA^{x3} at 7 mg/ml and 1 mM MLN8054 in DMSO. Crystals were briefly soaked in well buffer supplemented with 20% glycerol ($P3_1$) or 30% glycerol ($P6_122$) before flash freezing in liquid nitrogen.

In vitro kinase assays
Kinase assays were carried out at room temperature using a Labchip EZ Reader II system (Caliper Life Sciences) and a fluorescein-labelled substrate peptide (5-FAM-LRRASLG-CONH2) in a buffer of 50 mM Tris pH 7.5, 200 mM NaCl, 5 mM $MgCl_2$, 10% glycerol, 2% DMSO and 10 mM β-mercaptoethanol. 1 nM (AurA), 0.51 nM (AurA^{x3}), 0.15 nM (AurA^{TE}) or 0.4 nm (AurA^{WL}) enzyme in duplicate were pre-incubated in 25 µl reaction volume with 1.5 µM substrate peptide and stated concentration of MLN8054 for 10 mins before starting the reaction with stated concentrations of ATP. Measurements of substrate phosphorylation were taken every 5 mins for 1 hr (AurA, AurA^{TE} and AurA^{WL}) and 30 mins (AurA^{x3}). In the experiments to measure the effect of TPX2 on the potency of MLN8054, 3.4 µM TPX2 (residues 1-43) was pre-incubated with AurA for 10 mins before the addition of MLN8054 and substrate. This concentration is 340 times the EC_{50} of TPX2, which was determined to be 10 nM under conditions of saturating ATP. All measurements conformed to the linear initial rate assumption and best-fit rates were used to construct rate v [ATP] curves. Data were fitted to a global model for competitive inhibition using Prism5 (www.graphpad.com).

Crystallographic data processing and refinement
Diffraction data was reduced using Mosflm, scaled with Scala and the molecular replacement solutions were obtained with Phaser using the structure of ADP-bound Aurora-A as a model [21]. Four AurA^{x3} molecules were located in the $P3_1$ asymmetric unit, exhibiting clear difference density corresponding to two different conformations of the activation loop. Coordinates and refinement parameter (.cif) files for the MLN8054 ligand were made using Phenix [22]. Iterative cycles of model building and refinement were carried out using Coot and Phenix [21, 22]. All structure figures were produced using PyMOL (http://www.pymol.org).

Sequence analysis of the human kinome
The human ePK alignment containing 491 kinase domains, available at http://www.kinome.com, was used as the basis for calculating the frequency of amino acids at specific positions within the sequence as shown in Table 3 [23]. The sequence alignment was interrogated using a custom Perl script, available upon request.

Accession Codes

Coordinates and structure factors of AurA^{x3}/MLN8054 structures have been deposited in the Protein Data Bank (PDB) with accession code 2WTV ($P3_1$) and 2WTW ($P6_122$).

RESULTS

Characterisation of an active-site model of Aurora-B

The catalytic domains of human Aurora-A and Aurora-B are 76% identical at the primary sequence level, and differ by just three amino acids in their ATP-binding pockets - residues Leu215, Thr217 and Arg220 in Aurora-A are replaced by Arg159, Glu161, and Lys164 respectively in Aurora-B. To date, comparative studies have been frustrated because human Aurora-B has poor physico-chemical properties relative to Aurora-A and has not been crystallized. We constructed a triple point mutant version of the catalytic domain of Aurora-A (residues 122-403, Leu215Arg, Thr217Glu, Arg220Lys), which we call AurA^{x3}, as an Aurora-B active site mimic for crystallographic studies and to assess the contribution of the three residues to selectivity of MLN8054. The resulting enzyme is catalytically active, with kinetic parameters very similar to those for wild-type Aurora-A catalytic domain, which we call AurA (Figure 1a, Table 1). MLN8054 acts as an ATP-competitive inhibitor for both enzymes (Lineweaver-Burke plots intersecting on y-axis, data not shown) and the resultant K_is show a 6-fold discrimination for AurA over AurA^{x3}, greater than that which can be explained by the relative K_ms of the active site for ATP alone. This level of discrimination compares well with the 7-fold difference in dissociation constants reported in the absence of ATP using bead-based competition binding assays [14] although we report a consistently tighter binding (0.3 nM compared with 6.5 nM and 1.8 nM compared with 43 nM for Aurora-A and Aurora-B respectively). We have used equation (1) and our measured K_i to calculate the IC_{50} we would expect to measure for AurA under the experimental conditions reported for radioactive FlashPlate assays [13]. The calculated value of 3 nM compares very well with the published IC_{50} of 4 nM although we should point out that the extremely tight binding of MLN8054 means that the IC_{50} contains a large contribution from the assay enzyme concentration. A similar calculation for Aurora-B using the K_i for AurA^{x3} and a commercially reported K_m for Aurora-B (5 μM, http://www.caliperls.com/products/aurb-h.htm) is within a factor of two (calculated 93 nM, reported 172 nM).

$$IC_{50} = K_i\left(1+\frac{S}{K_m}\right)+\frac{[enzyme]}{2} \qquad (1)$$

We can thus conclude that the three point mutations differentiating AurA^{x3} and AurA provide a good model for assessing the contribution of active site residues to the binding of MLN8054. Interestingly, the difference between our measured K_m for ATP for AurA^{x3} (46 μM) and the reported value for AurB (5 μM) means that we would expect additional residues outside the active site pocket to influence the binding of ATP.

Binding mode of MLN8054 in the active site of Aurora kinase

The chemical structure of MLN8054 is shown in Figure 1b. AurA^{x3} was co-crystallised with MLN8054 and the structure determined to a resolution of 2.4 Å (Table 2). There are four AurA^{x3} molecules in the asymmetric unit that adopt two slightly different protein conformations of which chains A and B are representative (Figure 2a). The two conformations are the result of two different crystal packing contacts between the activation loop and a neighbouring molecule (stars in Figure 2a). The structure of Aurora-A catalytic domain mutated on the two sites of auto-phosphorylation (Thr287Ala, Thr288Ala), which we shall refer to as AurA^{AA}, bound to the 8054-like compound (shown in Figure 1b), has recently been determined (PDB code 3H10, [24]). This complex crystallized in a different crystal form ($P2_12_12_1$) to the AurA^{x3}/MLN8054 ($P3_1$). In chains A and B of this structure the activation loop of AurA^{AA} has a very similar conformation to that found in chain B of the AurA^{x3}/MLN8054 structure and is involved in different crystal packing contacts (Figure 2a). The activation loop is disordered between residues 284-291 in the third chain (D) of the AurA^{AA}/8054-like structure, which presumably cannot form a stabilizing crystal packing contact.

Additional electron density within the active site of AurA^{x3} was very clear, and the MLN8054 ligand was fitted unambiguously (Figure 2b). The two different conformations of AurA^{x3} are in fact very similar in the vicinity of MLN8054, with the exception of residue Glu217, one of the residues mutated to mimic Aurora-B. In chain A Glu217 is closest to the benzoic acid moiety of MLN8054 (3.8 Å shortest interatomic distance), whereas in chain B Glu217 is closest to the difluorophenyl group (4.7 Å shortest interatomic distance). The active site of AurA^{AA} bound to the 8054-like compound is very similar in all three chains and is very similar to that of either of the two chains of AurA^{x3} bound to MLN8054 (Figure 2b). In the structure of AurA^{AA}/8054-like, the methyl group of Thr217 is closest to the difluorophenyl group (3.6-3.8Å). The substitution of Glu for Thr at position 217 has no effect on the binding mode. However, the individual Thr217Glu point mutant of Aurora-A (AurA^{TE}) is almost 20-fold less potently inhibited by MLN8054 than the wild-type AurA (Figure 1, Table 1). The difference in potency of MLN8054 inhibition between AurA and AurA^{x3} is therefore primarily due to the Thr217Glu mutation. The difference is modest because there is no steric clash and hence no change in binding mode, and the flexibility of the Glu217 sidechain reduces the effectiveness of the repulsion between the ionised glutamate and the hydrophobic difluorophenyl or benzoic acid groups of MLN8054. With the exception of Glu217, the interactions between MLN8054 and AurA^{x3} chains A and B are identical, as are the contacts between AurA^{AA} and the 8054-like compound. MLN8054 forms two H-bonds with the hinge region of AurA^{x3} at Ala213, and a water-mediated H-bond to Asp274 (Figure 2c). The aromatic benzoic acid group sits above the C_α of Gly216 in a position similar to that occupied by aromatic rings in other Aurora inhibitor structures (e.g. PDB codes 2BFY [25], 2W1I [26]). The chlorine atom and the aromatic ring to which it is attached pack against the Gly-rich loop. The difluorophenyl group packs against Leu263, Ala273 and Val279, which also packs against the chlorine atom. With the exception of the acidic group, the entire molecule of MLN8054 is buried inside the active site pocket of AurA^{x3}. Remarkably, this is achieved in part by the remodeling of the activation loop conformation to wrap around part of the inhibitor.

The conformation of the activation loop induced by binding of MLN8054

The conformations of the activation loop adopted by AurA^{x3} bound to MLN8054 and AurA^{AA} bound to the 8054-like compound are highly unusual. The activation loop is flipped around compared to the DFG-in conformation observed in the ADP-bound AurA structure [20] and superficially resembles a DFG-out conformation, as observed in AurA/quinazoline-13 or cAbl bound to a Glivec variant (Figure 3a, PDB codes 2C6E and 1FPU respectively [3, 27]). Upon closer inspection, the conformation of the activation loop of AurA^{x3}/MLN8054 is clearly different. In DFG-in and DFG-out conformations of kinases, the aspartic acid and phenylalanine sidechains sit on opposite sides of the backbone. In these conformations, when the phenylalanine sidechain points into the interior of the protein, the aspartic acid sidechain points out into the active site and *vice versa* (Figure 3b). By contrast, in the AurA^{x3}/MLN8045 and AurA^{AA}/8054-like structures, both Asp274 and Phe275 project up into the interior of the kinase (Figure 3b,c). For this reason, and for the sake of brevity, we shall refer to this conformation as DFG-up.

The DFG-up conformation is characterized by a substantial reorganization of the activation loop between residues 274-293 and the HRD-motif at residues His254 and Arg255. Compared with the DFG-in conformation, the sidechain of Asp274 is rotated by approximately 180° so that it points into the interior of the protein, parallel to helix αC (Figure 3b). The sidechain of Phe275 points inwards and occupies a pocket above the Glu181 sidechain, whereas in the DFG-in conformation Phe275 occupies a pocket below Glu181. The Glu181 sidechain makes a H-bond with the indole ring of Trp277, which is twisted around from its outward position in the DFG-in conformation. Glu181 is a crucial residue for catalysis because it forms a salt bridge with Lys162 that positions the phosphates of ATP for transfer to substrate. In the DFG-up conformation, Lys162 forms a H-bond with Ser278 of the activation loop. Thus, although the salt bridge is broken in the DFG-up conformation, both residues find alternative partners with which to form H-bonds. The conformational change in the activation loop moves the C_α of Val279 approximately 19 Å compared to its position in the DFG-in structure. Val279 can thus make two points of contact with MLN8054/8054-like. Beyond Val279, the conformations of chains A and B deviate until the end of the activation loop (Leu293), and the differences are likely due to the different crystal packing contacts (Figure 2a). The sidechains of the HRD motif are switched in the DFG-up structure. His254 points outwards, whereas in the DFG-in conformation it usually points inwards and stacks against Phe275. Arg255 points inwards and interacts with Asp274 (DFG motif) and Asn185 (helix αC), whereas it normally faces outwards, and recognises the phosphorylated Thr288 in an active AurA structure (PDB code 1OL5 [20]).

The DFG-up conformation is distinct from the DFG-out conformation that is observed in the structures of quinazoline-13 bound to Aurora-A or a Glivec variant bound to cAbl. Apart from the differences in the DFG motif, in the DFG-out conformation Trp277 interacts with the quinazoline-13 inhibitor and the arrangement of the HRD-motif is similar to that found in the DFG-in conformation. Additionally, structures of Aurora-A and cAbl in the DFG-out conformation are of dephosphorylated kinases, whereas the DFG-up is observed with either phosphorylated or unphosphorylated Aurora-A. We speculate that phosphorylated Aurora-A can adopt DFG-up (and probably DFG-out) conformations without much energetic penalty because the

phosphorylated activation loop of Aurora-A is not stably locked in the active conformation except in the presence of TPX2 [20]. One prediction from the AurA^{x3}/MLN8054 structure is that the binding of TPX2 should decrease the potency of MLN8054 either through competition or because more energy is required to move the activation loop from its stable, active conformation into DFG-up. We determined the K_i for MLN8054 for AurA in the presence of a saturating concentration of TPX2 to be 3.3 ± 0.2 nM, a substantial increase on the K_i in the absence of TPX2 comparable to that obtained with AurA^{x3} or AurA^{TE} (Figure S1, Table 1, Table S1).

Insights into the selectivity of MLN8054 for Aurora kinases

Close inspection of the structure shows that many of the interactions between residues proximal to the active site are rearranged with respect to previous Aurora-A structures. This observation led us to consider whether other kinases might be able to adopt a similar conformation and if this might have any bearing on the selectivity of MLN8054. A search of the published alignment of human kinases and a search using the ProSite server reveals that only Aurora kinases possess a tryptophan at the equivalent position to 277, three residues after the start of the DFG motif (D+3, Table 3) [23]. Most of the more frequent residues at this position are hydrophobic and could not form a H-bond with Glu181. The exception to this is serine, found in 7.5% of kinases, although the position of the sidechain would have to be shifted by 2 Å to make the H-bond. In addition, Trp277 makes hydrophobic contacts with Phe144 and Val174 that could not be made by a serine sidechain. We mutated AurA at Trp277 to leucine, the most common residue at this position in human protein kinases. The K_i for MLN8054 for AurA^{WL} was determined to be 4.4 ± 0.4 nM, comparable to that determined for AurA^{x3} or AurA^{TE} (Figure S1, Table S1). This supports our suggestion that the unusual tryptophan residue at position 277 contributes to MLN8054 selectivity towards Aurora kinases. Val279 at D+5 is also unusual at its position in the kinase domain and is found in less than 5% of kinases (Table 3). In most kinases that are regulated by phosphorylation of the activation loop the equivalent residue at this sequence position is most frequently a lysine or arginine, which interacts with the activating phosphate group (i.e. on a residue equivalent to Thr288) and helps order the activation loop. Full ordering of the activation loop of Aurora-A proceeds by a different mechanism than most kinases because binding of an activator such as TPX2 is required in addition to phosphorylation on Thr288 [20]. The interior surface of Aurora kinases that is contacted by the DFG motif in the DFG-up conformation is highly unusual. In most kinases, this region is hydrophobic, and in particular there is a conserved hydrophobic residue on the αC helix that forms part of the hydrophobic spine of kinases and interacts with the Phe sidechain of the DFG motif in the DFG-in conformation [28]. Across all human kinases, this residue is a leucine in 53% of cases, and a methionine in 25%. In the Aurora family, this hydrophobic residue is replaced by Gln185, which makes a H-bond with the backbone at Leu194. The presence of Gln185 is presumably important for the DFG-up conformation because it lies at the centre of a network of polar interactions that involves the sidechains of Asp274, Arg255 and the backbone at Leu194. Only COT, a mitogen-activated protein kinase kinase kinase, has both equivalent identical residues to Gln185 and Val279, and no other kinase has even a related combination (Ile or Leu for Val, His or Asn for Gln). The Aurora family thus has a unique set of features that create the capacity to adopt the MLN8054-bound activation loop conformation: the presence of the polar back pocket, the lack of a basic residue at D+5 and the tryptophan at D+3. This

suggests that the conformation of AurA^{x3} bound to MLN8054 might not be easily accessible to other kinases, and might thus contribute to the selectivity of MLN8054.

A model to explain the structural and chemical basis for the conformational changes in DFG-out and DFG-up conformations of Aurora-A

We obtained a second crystal structure of the complex at 3.3Å resolution (AurA^{x3}/MLN8054*) in a *P*6$_1$22 crystal form that is very commonly obtained with AurA (Table 2). In this structure, the activation loop adopts a DFG-in conformation (Figure 4a, b). This may simply represent a crystallization artefact, because the crystal packing is incompatible with the DFG-up conformation of the activation loop, which appears to be trapped in the DFG-in conformation by crystal packing contacts. When compared to the ADP-bound AurA structure, there is a steric clash between the Gly-rich loop in the ADP-bound conformation and MLN8054 (star, Figure 4b). In the AurA^{x3}/MLN8054* structure the Gly-rich loop is displaced upwards due to contacts between MLN8054 and the Gly-rich loop at the sidechain at Val147 and the mainchain at residues 140-141 (Figure 4b). The AurA^{x3}/MLN8054* structure shows that the MLN8054 can be accommodated in the active site without movement of the activation loop, but requires displacement of the Gly-rich loop. Superposition of the higher resolution AurA^{x3}/MLN8054 or AurA^{AA}/8054-like structures show the same steric clash between the Gly-rich loop of the ADP-bound structure with MLN8054 and a second steric clash between the Gly-rich loop of the ADP-bound structure (at residues 142-143) with the activation loop of the MLN8054-bound structure at Val279 (Figure 4c). The higher resolution structures show a displacement of the Gly-rich loop similar to that observed at low resolution in the AurA^{x3}/MLN8054* structure. It appears that the upwards movement of the Gly-rich loop is a necessary adjustment to accommodate the activation loop in the DFG-up conformation, and could be an initial first step upon binding of MLN8054 to Aurora-A.

The fact that the DFG-up conformation has not been reported before suggested to us that there is something unusual about the binding of MLN8054 that induces this conformation. The superposition of AurA/ADP with AurA^{x3}/MLN8054 shows that the difluorophenyl group of MLN8054 occupies the equivalent space to that occupied by the α-PO_4 group of ADP, which we shall refer to as the α-PO_4 space (Figure 4d). The two groups have vastly different chemical properties, and the properties of this space are altered between DFG-in and DFG-up conformations. In the DFG-in conformation, Asp274 sits to one side of the α-PO_4 space and together with Asn261 coordinates two divalent cations (e.g. Mg^{2+}) that stabilise the ADP/ATP phosphates. In the DFG-up conformation, Asp274 is flipped and the Mg^{2+} binding sites are eliminated. The movement of Val279 completes the conversion of the α-PO_4 space to a hydrophobic pocket, which is occupied by the difluorophenyl group of MLN8054 (Figure 3b, 4d). The DFG-up conformation of Aurora-A could therefore be driven by the occupation of the α-PO_4 space by the difluorophenyl group of MLN8054.
Interestingly, a similar change to the chemical properties of the α-PO_4 space occurs in the DFG-out conformation. In fact, the DFG-up and DFG-out conformations are clearly related and they possess two equivalent hydrophobic pockets that can be filled by a phenyl group (yellow, green dashed circles Figure 4e). The groups which occupy these two pockets in the DFG-up or DFG-out conformations display a degree of symmetry. In the DFG-out conformation, the α-PO_4 space is occupied by the Phe275 sidechain and the second pocket is filled by the quinazoline-13 compound (Figure 3b,

4e). In the DFG-up conformation, the α-PO_4 space is occupied by the difluorophenyl group of MLN8054 and the second pocket is filled by the sidechain of Phe275. Further exploration of the chemical, structural and biophysical relationship between these two conformations may be beneficial in the production of more selective Aurora compounds.

DISCUSSION

The observation of the same, unusual activation loop conformation induced by two similar compounds bound to variants of the protein which are unphosphorylated ($AurA^{AA}$) or phosphorylated with mutations in the active site ($AurA^{x3}$), and which were crystallized in two different crystals forms, is strong evidence that this conformation is neither an artefact of any of the protein modifications nor an artefact of crystal packing, but is driven by binding of the MLN8054/8054-like compounds. This raises the concern that selectivity testing for MLN8054 may be difficult to interpret because the inhibitor might be expected to bind more tightly to off-target kinases in the inactive state rather than the active proteins which are used in assay screens. Our analysis of the sequence requirements for the DFG-up conformation raises the question of how MLN8054 is able to inhibit several other kinases, albeit with lower potency than the Aurora family, such as Abl (76% inhibition at 1 μM) and Yes (80% inhibition at 1 μM) [13]. It is possible that these kinases are able to adopt the DFG-up conformation, and that the lower potency is partly because this conformation is a less favoured, higher energy state. Alternatively, MLN8054 could bind to these kinases in a different conformation, such as the DFG-in conformation observed in the low-resolution $AurA^{x3}$/MLN8054* structure. The determination of the selectivity profile of this class of inhibitor is therefore perhaps most accurately achieved by using a direct binding screen against inactive and active forms of the kinases[14]. Rational design and prediction of selectivity profiles remains an extremely difficult challenge given the existence of multiple inactive conformations accessible to protein kinases and the possibility that some compounds might be able to target more than one conformation.

It has been suggested that Thr217 might be the basis for the higher potency of MLN8054 for Aurora-A over Aurora-B[24]. We have now confirmed that Thr217 is the main determinant of its bias towards Aurora-A *in vitro* and shown the relative disposition of a glutamic acid sidechain at this position in the crystal stucture. MLN8054 does not fully utilize the potential of the Thr217Glu substitution to generate selectivity, because the compound does not sit very close to residue 217 and can still be accommodated when the residue is substituted for glutamic acid. The selectivity of MLN8054 for Aurora-A over Aurora-B *in vitro* is not high, only approximately 6-fold using strictly comparable K_i or K_d measurements. In contrast, MLN8054 is over 100-fold selective for Aurora-A over Aurora-B in cell-based assays and the compound can be used to obtain a cellular phenotype consistent with clear discrimination [13, 29]. The Aurora-A activator TPX2 reduces the potency of MLN8054 versus Aurora-A, although only a specific pool of Aurora-A localized to mitotic spindle microtubules is thought to be bound to TPX2. The cellular potency of Aurora-A might be due to targeting the non-TPX2-bound pool of Aurora-A. The mechanism by which Aurora-B is only poorly inhibited by MLN8054 in cells is presently unclear. It is possible that Aurora-B is prevented from adopting the DFG-up conformation through binding to a protein partner, but it is not obvious how this could

be mediated from current structures of the Aurora-B/INCENP complex. The elucidation of this mechanism may be important for understanding the cellular regulation of these kinases.

The structure of AurA^{x3} bound to MLN8054 suggests that the specificity of this compound for the Aurora family is at least partly a function of the protein conformation it induces. This does not imply that we believe it to be impossible to produce inhibitors that target other kinases in a DFG-up conformation. On the contrary, it might be possible to exploit the principle behind the DFG-up conformation to generate compounds that induce the DFG-up conformation of other kinases, just as it has been possible to generate potent inhibitors that bind the DFG-out conformation of a number of kinases. This is because the conformation induced by these compounds would be DFG-up, but would differ in the precise details of the conformation adopted by the activation loop, especially the residues just after the DFG motif. One feature that is potentially vital for adopting a DFG-up conformation is the polar residue on the C-helix (Gln185), and an equivalent polar residue is present in just under 10% of human kinases. We predict that these would be the most likely targets for DFG-up inhibitors. The other key features of the DFG-up conformation are the interactions within the kinase domain and between the activation loop at D+5 (Val279) and the inhibitor. To design a DFG-up targeting inhibitor, we predict that one should modify a Type I inhibitor with the addition of a hydrophobic group to fit the α-PO_4 pocket that is complementary to the residue at D+5. One might expect that this would only work with kinases that possess residues at D+3 and D+4 capable of making compensating interactions with the disrupted Lys-Glu salt bridge residues. Future studies will elaborate which other kinases can be induced to form the DFG-up conformation. Furthermore, the discovery of the DFG-up conformation, and our recent discovery of multiple, stable, ligand-induced conformations of Nek2 kinase [30] suggest to us that the conformational space of the activation loop should be further explored, and exploited to produce selective inhibitors.

AUTHOR CONTRIBUTION

Charlotte Dodson carried out the enzyme kinetics studies, contributed to the interpretation of kinetic data and contributed to the writing of the paper. Magda Kosmopoulou prepared the proteins, generated crystals, determined the X-ray crystal structures and contributed to the interpretation of structural data. Mark Richards carried out DNA manipulations and mutagenesis. Butrus Atrash synthesized the MLN8054 compound. Vassilios Bavetsias advised on the design of the synthetic route to MLN8054 and contributed to the interpretation of data in relation to MLN8054 Aurora isoform selectivity. Julian Blagg provided leadership in the generation of MLN8054 and contributed to the interpretation of data in relation to MLN8054 Aurora isoform selectivity. Richard Bayliss was the principal investigator on the project, contributed to the X-ray crystal structure determination, interpreted the data and wrote the paper.

ACKNOWLEDGEMENTS

We are indebted to the staff of ESRF beamlines ID14.1 and ID14.4 for their support during data collection. We wish to thank our colleagues at The Institute of Cancer Research for their helpful comments and support, especially Wynne Aherne, Kathy

Boxall, Ian Collins, Amir Faisal, Spiros Linardopoulos and Rob van Montfort at the Centre for Cancer Therapeutics. The authors are employees of The Institute of Cancer Research which has a commercial interest in a number of drug discovery programs for which further information is available from the ICR Enterprise Unit. Julian Blagg is a consultant and stock holder of both Pfizer and Solace Pharmaceuticals.

FUNDING

This study was supported by a Royal Society University Research Fellowship, the Career Development Faculty Programme of The Institute of Cancer Research, a Cancer Research UK project grant (C24461/A8032) and a Breakthrough Breast Cancer project grant (AURA 05/06) to R.B., and the core Cancer Research UK support to the Centre for Cancer Therapeutics (C309/A8274) to J.B. We acknowledge infrastructural support for structural biology at The Institute of Cancer Research by Cancer Research UK and NHS funding to the National Institute for Health Research (NIHR) Biomedical Research Centre.

FIGURE LEGENDS

Figure 1. Comparison of AurA, AurA^{x3} and AurA^{TE} kinetic parameters and MLN8054 inhibition

a) Global fits of apparent ATP K_m in presence of varying concentrations of MLN8054: 0 nM (black), 0.02 nM (dark grey, AurA only), 0.06 (light grey, AurA^{x3} and AurA^{TE} only, filled circles), 0.2 nM (black), 0.6 nM (dark grey), 2 nM (light grey, open circles), 5 nM (black), 16 nM (dark grey), 50 nM (light grey, AurA^{x3} and AurA^{TE} only, diamonds). Error bars and quoted errors are fitting errors of duplicate measurements. The average of three repeat measurements in duplicate for AurA^{x3} did not alter the K_i or K_m, and standard errors of these values were the same magnitude as fitting errors quoted.

b) Chemical structures of MLN8054, the 8054-like compound [24] and quinazoline-13 [27].

Figure 2. Binding mode of MLN8054

a) Two different conformations of AurA^{x3} are shown as yellow cartoons, with MLN8054 shown as spheres using the colour scheme carbon grey, nitrogen blue, oxygen red, chlorine green and fluorine cyan. The structure of AurA^{AA} is shown as an orange cartoon, with the 8054-like compound shown in the same colour scheme as MLN8054. Crystal contacts that direct the different paths of activation loops are marked with stars, and the neighbouring protein molecule is depicted as grey cartoon.

b) Magnified view of the active site. The mainchain of AurA^{x3}/AurA^{AA} is shown as a C_α trace. MLN8054/8054-like and residues lining the active site of AurA^{x3}/AurA^{AA} are shown in stick representation. The final $2mF_o$-dF_c electron density map around MLN8054 is shown as a wiremesh contoured at 1.0σ.

c) Magnified view of the active site shown in a view rotated through approximately 90° about the horizontal axis relative to (b). Putative H-bonds are shown as dashed lines, and an ordered water molecule that mediates contact between the ligand and the protein is shown as a red sphere. The sidechain of Tyr212 is omitted so that the H-bonds between Ala213 and the ligand are not obscured.

Figure 3. Comparison of the activation loop conformations in the AurA^{x3}/MLN8054 structure with those of DFG-in and DFG-out structures

a) Cartoon representation of kinase structures with the activation loop highlighted in magenta and the ligand shown as grey spheres. From top to bottom the structures shown are AurA^{x3}/MLN8054 (chain A), AurA/ADP (PDB code 1OL7 [20]), AurA/quinazoline-13 (PDB code 2C6E [27]), and cABL/Glivec variant (PDB code 1FPU [3]).

b) Magnified stereo views of the active site of AurA^{x3}/MLN8054 (chain A), AurA/ADP and AurA/quinazoline-13 in the same orientation as in (a). The N-terminal residues of the activation loop (ADFGWSV), the HRD-motif residues and the two residues that form an important salt bridge in the active enzyme (Lys162-Glu181) are shown in stick representation.

c) Magnified stereo view of AurA^{x3}/MLN8054 (chain A) oriented to give a clear view of the interactions between the activation loop residues and the interior of the protein. The backbone of AurA^{x3} is shown as a C_α trace, key residues and MLN8054 are shown in stick representation.

Figure 4. Activation loop conformational differences between Aurora-A structures are perhaps driven by the chemical group that occupies the α-PO4 space

a) Superposition of AurA/ADP (protein dark teal cartoon, ADP dark teal sticks, PDB code 1OL7 [20]) with the 3.3 Å resolution AurA^{x3}/MLN8054* structure (protein pink cartoon, MLN8054 pink sticks).

b) Magnified view of the superposition, with mainchain shown as ribbon and key residues shown as sticks and the ADP molecule omitted for clarity. The final $2mF_o$-dF_c electron density map around MLN8054 is shown as a wiremesh contoured at 1.0σ. The steric clash between the Gly-rich loop (shown as a thicker ribbon) in the ADP-bound structure and MLN8054 is highlighted with a black star.

c) Superposition of chain A of AurA^{x3}/MLN8054 structure (chain A, protein yellow ribbon, MLN8054 grey sticks) with structure of phosphorylated, ADP-bound AurA (protein dark teal ribbon, ADP dark teal sticks, PDB code 1OL7 [20]). Key regions of conformational difference are marked.

d) Magnified view of superposition to show detail of active site. The upper panel is depicted in the same orientation as (c), the view in the lower panel is rotated through 90º about the vertical axis. Steric clashes between MLN8054 or the activation loop of MLN8054-bound AurA^{x3} and the Gly-rich loop of ADP-bound AurA are highlighted with single and double stars respectively. Magnesium ions in the ADP-bound structure are depicted as spheres. In the lower panel, the deviation between the two structures starting from Asp274 in the activation loop is clearly evident.

e) Comparison of the phenyl-binding pockets of the three different DFG motif conformations. The left-hand images show simplified structural models of the three conformations viewed from the back of the active site looking out to solvent (i.e. 180º rotation relative to the top panel of Figure 4d). The mainchain of the DFG motif is shown as a magenta cartoon, the Asp274 sidechain is shown as magenta space-filling, the sidechain of Phe275 as dark grey space-filling and the ligand as space-filling with the following colour scheme: carbon light grey, nitrogen blue, oxygen red, phosphorous orange, fluorine cyan. The right-hand images show a schematic diagram of the comparison. The α-PO_4 space is shown as a dashed yellow circle and the second phenyl-binding space is shown as a dashed green circle. The pocket occupied

by Phe275 in the DFG-in conformation does not coincide with the other two pockets and is shown as a dashed black circle. The aspartic acid and phenylalanine residues of the DFG motif are depicted with magenta and black lines respectively. Relevant features of the three ligands are shown as follows: the two phosphate groups of ADP as red stars; the terminal phenyl group of quinazoline-13 as a grey hexagon; the difluorophenyl group of MLN8054 as a modified grey hexagon.

REFERENCES

1 Zhang, J., Yang, P. L. and Gray, N. S. (2009) Targeting cancer with small molecule kinase inhibitors. Nat. Rev. Cancer. 9, 28-39

2 van Montfort, R. L. and Workman, P. (2009) Structure-based design of molecular cancer therapeutics. Trends Biotechnol. 27, 315-328

3 Schindler, T., Bornmann, W., Pellicena, P., Miller, W. T., Clarkson, B. and Kuriyan, J. (2000) Structural mechanism for STI-571 inhibition of abelson tyrosine kinase. Science. 289, 1938-1942

4 Pargellis, C., Tong, L., Churchill, L., Cirillo, P. F., Gilmore, T., Graham, A. G., Grob, P. M., Hickey, E. R., Moss, N., Pav, S. and Regan, J. (2002) Inhibition of p38 MAP kinase by utilizing a novel allosteric binding site. Nat. Struct. Biol. 9, 268-272

5 Wan, P. T., Garnett, M. J., Roe, S. M., Lee, S., Niculescu-Duvaz, D., Good, V. M., Jones, C. M., Marshall, C. J., Springer, C. J., Barford, D. and Marais, R. (2004) Mechanism of activation of the RAF-ERK signaling pathway by oncogenic mutations of B-RAF. Cell. 116, 855-867

6 Liu, Y. and Gray, N. S. (2006) Rational design of inhibitors that bind to inactive kinase conformations. Nat. Chem. Biol. 2, 358-364

7 Seeliger, M. A., Nagar, B., Frank, F., Cao, X., Henderson, M. N. and Kuriyan, J. (2007) c-Src binds to the cancer drug imatinib with an inactive Abl/c-Kit conformation and a distributed thermodynamic penalty. Structure. 15, 299-311

8 Dar, A. C., Lopez, M. S. and Shokat, K. M. (2008) Small molecule recognition of c-Src via the Imatinib-binding conformation. Chem. Biol. 15, 1015-1022

9 Jackson, J. R., Patrick, D. R., Dar, M. M. and Huang, P. S. (2007) Targeted anti-mitotic therapies: can we improve on tubulin agents? Nat. Rev. Cancer. 7, 107-117

10 Keen, N. and Taylor, S. (2004) Aurora-kinase inhibitors as anticancer agents. Nat. Rev. Cancer. 4, 927-936

11 Pollard, J. R. and Mortimore, M. (2009) Discovery and development of aurora kinase inhibitors as anticancer agents. J. Med. Chem. 52, 2629-2651

12 Bavetsias, V., Sun, C., Bouloc, N., Reynisson, J., Workman, P., Linardopoulos, S. and McDonald, E. (2007) Hit generation and exploration: imidazo[4,5-b]pyridine derivatives as inhibitors of Aurora kinases. Bioorg. Med. Chem. Lett. 17, 6567-6571

13 Manfredi, M. G., Ecsedy, J. A., Meetze, K. A., Balani, S. K., Burenkova, O., Chen, W., Galvin, K. M., Hoar, K. M., Huck, J. J., LeRoy, P. J., Ray, E. T., Sells, T. B., Stringer, B., Stroud, S. G., Vos, T. J., Weatherhead, G. S., Wysong, D. R., Zhang, M., Bolen, J. B. and Claiborne, C. F. (2007) Antitumor activity of MLN8054, an orally active small-molecule inhibitor of Aurora A kinase. Proc. Natl. Acad. Sci. U.S.A. 104, 4106-4111

14 Karaman, M. W., Herrgard, S., Treiber, D. K., Gallant, P., Atteridge, C. E., Campbell, B. T., Chan, K. W., Ciceri, P., Davis, M. I., Edeen, P. T., Faraoni, R., Floyd, M., Hunt, J. P., Lockhart, D. J., Milanov, Z. V., Morrison, M. J., Pallares, G., Patel, H. K., Pritchard, S., Wodicka, L. M. and Zarrinkar, P. P. (2008) A quantitative analysis of kinase inhibitor selectivity. Nat. Biotechnol. 26, 127-132

15 Jeng, Y. M., Peng, S. Y., Lin, C. Y. and Hsu, H. C. (2004) Overexpression and amplification of Aurora-A in hepatocellular carcinoma. Clin. Cancer Res. 10, 2065-2071

16 Zhou, H., Kuang, J., Zhong, L., Kuo, W. L., Gray, J. W., Sahin, A., Brinkley, B. R. and Sen, S. (1998) Tumour amplified kinase STK15/BTAK induces centrosome amplification, aneuploidy and transformation. Nat. Genet. 20, 189-193

17 Ewart-Toland, A., Briassouli, P., de Koning, J. P., Mao, J. H., Yuan, J., Chan, F., MacCarthy-Morrogh, L., Ponder, B. A., Nagase, H., Burn, J., Ball, S., Almeida, M., Linardopoulos, S. and Balmain, A. (2003) Identification of Stk6/STK15 as a candidate low-penetrance tumor-susceptibility gene in mouse and human. Nat. Genet. 34, 403-412

18 Greenman, C., Stephens, P., Smith, R., Dalgliesh, G. L., Hunter, C., Bignell, G., Davies, H., Teague, J., Butler, A., Stevens, C., Edkins, S., O'Meara, S., Vastrik, I., Schmidt, E. E., Avis, T., Barthorpe, S., Bhamra, G., Buck, G., Choudhury, B., Clements, J., Cole, J., Dicks, E., Forbes, S., Gray, K., Halliday, K., Harrison, R., Hills, K., Hinton, J., Jenkinson, A., Jones, D., Menzies, A., Mironenko, T., Perry, J., Raine, K., Richardson, D., Shepherd, R., Small, A., Tofts, C., Varian, J., Webb, T., West, S., Widaa, S., Yates, A., Cahill, D. P., Louis, D. N., Goldstraw, P., Nicholson, A. G., Brasseur, F., Looijenga, L., Weber, B. L., Chiew, Y. E., DeFazio, A., Greaves, M. F., Green, A. R., Campbell, P., Birney, E., Easton, D. F., Chenevix-Trench, G., Tan, M. H., Khoo, S. K., Teh, B. T., Yuen, S. T., Leung, S. Y., Wooster, R., Futreal, P. A. and Stratton, M. R. (2007) Patterns of somatic mutation in human cancer genomes. Nature. 446, 153-158

19 Claiborne, C. F. P., Lloyd J.; Boyce, Richard J.; Sells, Todd B.; Stroud, Stephen G.; Travers, Stuart; Vos, Tricia J.; Weatherhead, Gabriel S. (2005) Preparation of pyrimidoazepine derivatives and methods for inhibiting mitotic progression. US 2005256102 A1

20 Bayliss, R., Sardon, T., Vernos, I. and Conti, E. (2003) Structural basis of Aurora-A activation by TPX2 at the mitotic spindle. Mol. Cell. 12, 851-862

21 CCP4. (1994) The CCP4 (Collaborative Computational Project Number 4) suite: programmes for protein crystallography. Acta Crystallogr. D Biol. Crystallogr. 50, 760-763

22 Adams, P. D., Grosse-Kunstleve, R. W., Hung, L. W., Ioerger, T. R., McCoy, A. J., Moriarty, N. W., Read, R. J., Sacchettini, J. C., Sauter, N. K. and Terwilliger, T. C. (2002) PHENIX: building new software for automated crystallographic structure determination. Acta Crystallogr. D Biol. Crystallogr. 58, 1948-1954

23 Manning, G., Whyte, D. B., Martinez, R., Hunter, T. and Sudarsanam, S. (2002) The protein kinase complement of the human genome. Science. 298, 1912-1934

24 Aliagas-Martin, I., Burdick, D., Corson, L., Dotson, J., Drummond, J., Fields, C., Huang, O. W., Hunsaker, T., Kleinheinz, T., Krueger, E., Liang, J., Moffat, J., Phillips, G., Pulk, R., Rawson, T. E., Ultsch, M., Walker, L., Wiesmann, C., Zhang, B., Zhu, B. Y. and Cochran, A. G. (2009) A class of 2,4-bisanilinopyrimidine Aurora A inhibitors with unusually high selectivity against Aurora B. J. Med. Chem. 52, 3300-3307

25 Sessa, F., Mapelli, M., Ciferri, C., Tarricone, C., Areces, L. B., Schneider, T. R., Stukenberg, P. T. and Musacchio, A. (2005) Mechanism of Aurora B activation by INCENP and inhibition by hesperadin. Mol. Cell. 18, 379-391

26 Howard, S., Berdini, V., Boulstridge, J. A., Carr, M. G., Cross, D. M., Curry, J., Devine, L. A., Early, T. R., Fazal, L., Gill, A. L., Heathcote, M., Maman, S., Matthews, J. E., McMenamin, R. L., Navarro, E. F., O'Brien, M. A., O'Reilly, M., Rees, D. C., Reule, M., Tisi, D., Williams, G., Vinkovic, M. and Wyatt, P. G. (2009) Fragment-based discovery of the pyrazol-4-yl urea (AT9283), a multitargeted kinase inhibitor with potent aurora kinase activity. J. Med. Chem. 52, 379-388

27 Heron, N. M., Anderson, M., Blowers, D. P., Breed, J., Eden, J. M., Green, S., Hill, G. B., Johnson, T., Jung, F. H., McMiken, H. H., Mortlock, A. A., Pannifer, A. D., Pauptit, R. A., Pink, J., Roberts, N. J. and Rowsell, S. (2006) SAR and inhibitor complex structure determination of a novel class of potent and specific Aurora kinase inhibitors. Bioorg. Med. Chem. Lett. 16, 1320-1323

28 Kornev, A. P., Haste, N. M., Taylor, S. S. and Eyck, L. F. (2006) Surface comparison of active and inactive protein kinases identifies a conserved activation mechanism. Proc. Natl. Acad. Sci. U.S.A. 103, 17783-17788

29 LeRoy, P. J., Hunter, J. J., Hoar, K. M., Burke, K. E., Shinde, V., Ruan, J., Bowman, D., Galvin, K. and Ecsedy, J. A. (2007) Localization of human TACC3 to mitotic spindles is mediated by phosphorylation on Ser558 by Aurora A: a novel pharmacodynamic method for measuring Aurora A activity. Cancer Res. 67, 5362-5370

30 Westwood, I., Cheary, D. M., Baxter, J. E., Richards, M. W., van Montfort, R. L., Fry, A. M. and Bayliss, R. (2009) Insights into the conformational variability and regulation of human Nek2 kinase. J. Mol. Biol. 386, 476-485

Table 1. Summary of parameters determined for kinase activity and inhibition by MLN8054

	AurA	AurA^{x3}	AurA^{TE}
$K_{m,\ ATP}$ (μM)	20 ± 2	46 ± 3	72 ± 5
k_{cat} (min^{-1})[a]	4.8 ± 0.7	8.1 ± 1.2	52.4 ± 7.5
K_i (nM)	0.27 ± 0.03	1.8 ± 0.2	5.2 ± 0.3

a) Errors on k_{cat} are propagated from the fitting error on V_{max}, assuming a 10% error in the determination of the final concentrations of enzyme and peptide. The K_m for ATP for AurA is in excellent agreement with the previously published value [30].

Table 2. Summary of crystallographic analysis

Crystals		AurA^{x3}/MLN8054	AurA^{x3}/MLN8054*
Spacegroup		$P3_1$	$P6_122$
Lattice constants	*a* (Å)	118.71	84.04
	b (Å)	118.71	84.04
	c (Å)	135.89	171.06
Data collection			
Resolution range (Å)		59.3 - 2.4	72.9 - 3.3
(Highest resolution shell)		(2.53 - 2.40)	(3.30-3.48)
Unique reflections		83351 (11952)	5790 (815)
Completeness(%)		99.5 (97.6)	99.6 (99.5)
Multiplicity		3.4 (2.7)	14.8 (14.8)
Rmerge (%)		8.3 (34.6)	11.6 (46.7)
I/σ(I)		12.3 (3.2)	20.6 (7.7)
Refinement			
Resolution range		19.8 - 2.4	67 - 3.3
Number of reflections		79178	5738
*R*factor (%)		16.4	23.4
*R*free[a] (%)		21.1	28.8
R.m.s. deviations			
Bond lengths (Å)		0.005	0.004
Bond Angles (°)		1.05	0.820
Ramachandran outliers (%)		0.0	0.4
Ramachandran favoured (%)		98.4	92.9

[a] Free *R*factor was computed using 5% of the data assigned randomly.

Biochemical Journal Immediate Publication. Published on 12 Jan 2010 as manuscript BJ20091530

Table 3. Frequency of amino acids in the N-terminus of human kinase domain activation loops

Aurora-A kinase residue numbering

D	D+1	D+2	D+3	D+4	D+5
274	275	276	277	278	279
Frequency of occurrence in human ePK kinase domain sequences[1]					
Asp (458)	**Phe** (403)	**Gly** (446)	Leu (245)	Asp (247)	Arg (157)
	Leu (50)		Phe (58)	**Ser** (144)	Lys (109)
	Tyr (18)		Ser (37)	Cys (42)	Thr (33)
			Met (34)	Thr (18)	Ala (30)
			Val (31)	Gly (15)	**Val** (23)
			Ile (23)		Ser (22)
			.		Cys (16)
			.		Asn (16)
			Trp (3)		Leu (13)

1) Only residues that occur in more than 10 kinase domains are shown, with the exception of Trp at position 277. Aurora kinase residues are marked in bold and underlined.

Biochemical Journal Immediate Publication. Published on 12 Jan 2010 as manuscript BJ20091530

a

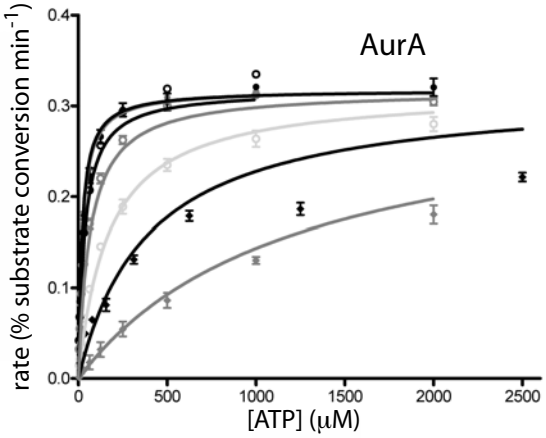

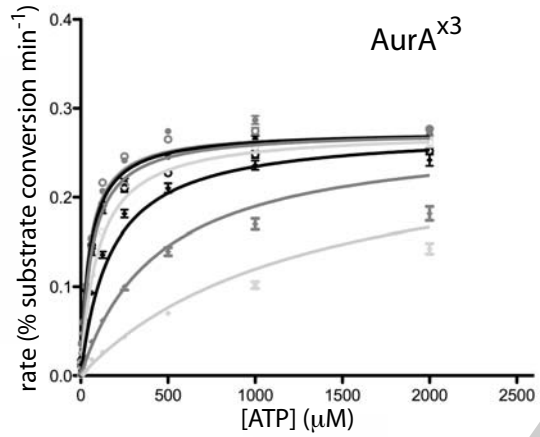

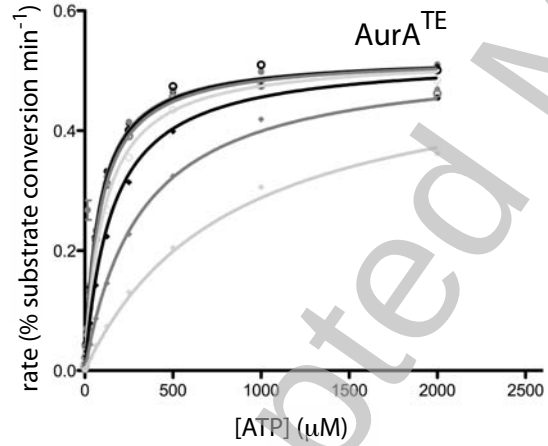

b

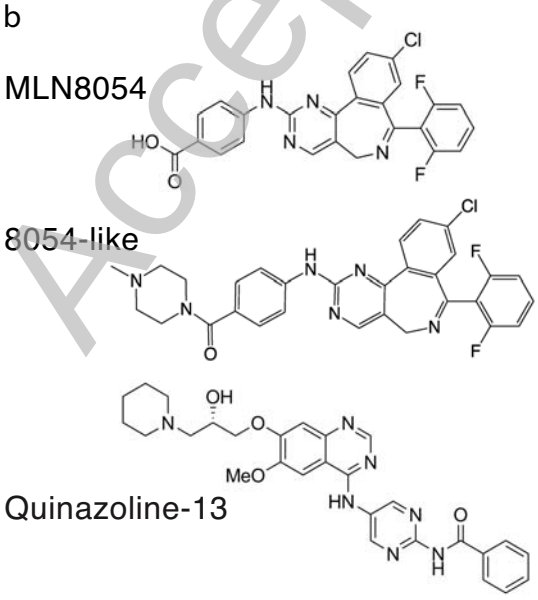

Biochemical Journal Immediate Publication. Published on 12 Jan 2010 as manuscript BJ20091530

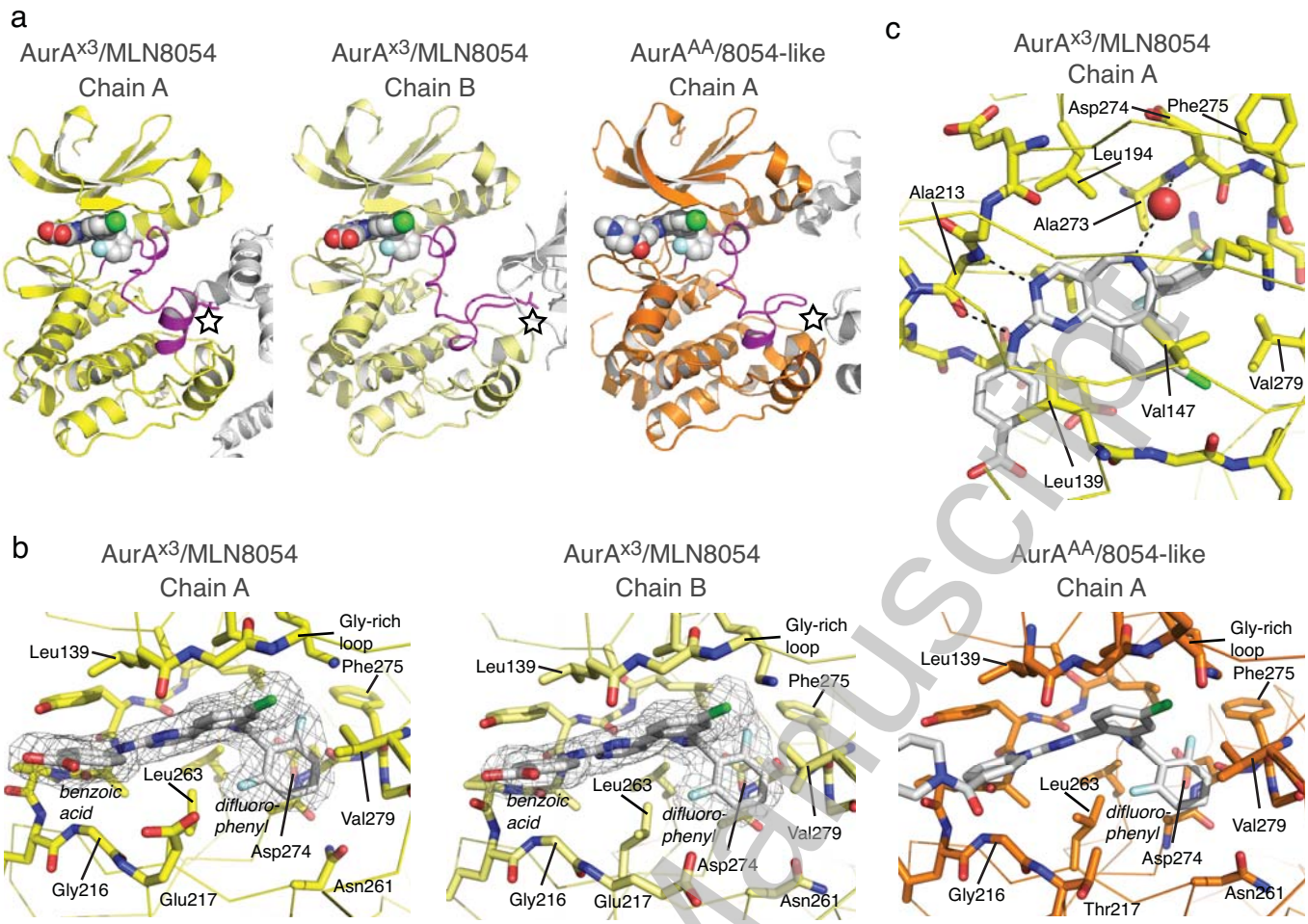

Biochemical Journal Immediate Publication. Published on 12 Jan 2010 as manuscript BJ20091530

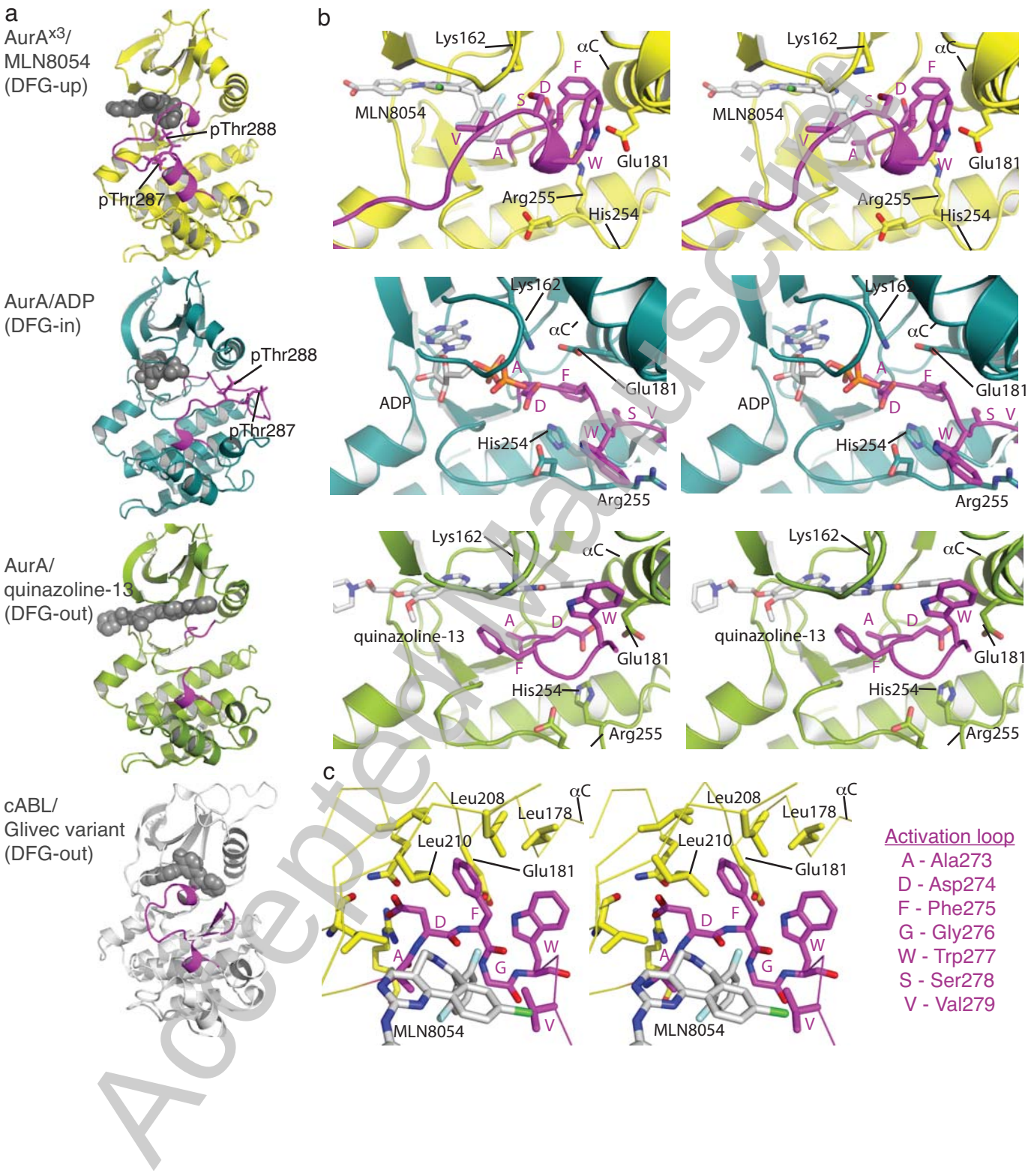

Biochemical Journal Immediate Publication. Published on 12 Jan 2010 as manuscript BJ20091530